

Accepted Manuscript

Carbenoid transfer reactions catalyzed by a ruthenium porphyrin macrocycle

Onno I. van den Boomen, Ruud G.E. Coumans, Niels Akeroyd, Theo P.J. Peters, Paul P.J. Schlebos, Jan Smits, René de Gelder, Johannes A.A.W. Elemans, Roeland J.M. Nolte, Alan E. Rowan



PII: S0040-4020(17)30510-0

DOI: [10.1016/j.tet.2017.05.035](https://doi.org/10.1016/j.tet.2017.05.035)

Reference: TET 28701

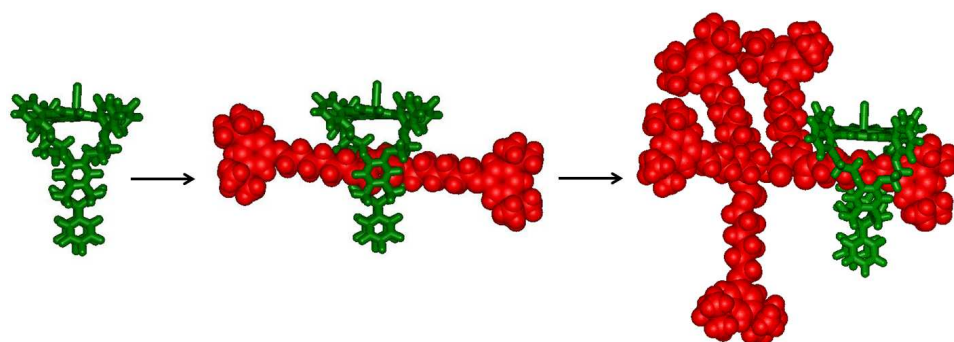
To appear in: *Tetrahedron*

Received Date: 8 April 2017

Accepted Date: 8 May 2017

Please cite this article as: van den Boomen OI, Coumans RGE, Akeroyd N, Peters TPJ, Schlebos PPJ, Smits J, de Gelder René, Elemans JAAW, Nolte RJM, Rowan AE, Carbenoid transfer reactions catalyzed by a ruthenium porphyrin macrocycle, *Tetrahedron* (2017), doi: 10.1016/j.tet.2017.05.035.

This is a PDF file of an unedited manuscript that has been accepted for publication. As a service to our customers we are providing this early version of the manuscript. The manuscript will undergo copyediting, typesetting, and review of the resulting proof before it is published in its final form. Please note that during the production process errors may be discovered which could affect the content, and all legal disclaimers that apply to the journal pertain.



ACCEPTED MANUSCRIPT

Carbenoid transfer reactions catalyzed by a ruthenium porphyrin macrocycle

Onno I. van den Boomen^a, Ruud G. E. Coumans^a, Niels Akeroyd^a, Theo P. J. Peters^a, Paul P. J. Schlebos^a, Jan Smits^a, René de Gelder^a, Johannes A. A. W. Elemans^{a,*},
Roeland J. M. Nolte^{a,*}, and Alan E. Rowan^{a,*}

^aRadboud University, Institute for molecules and Materials, Heyendaalseweg 135, 6525 AJ Nijmegen, The Netherlands

^bAustralian Institute for Bioengineering and Nanotechnology (AIBN), The University of Queensland, Brisbane QLD 4072, Australia

Email: J.Elemans@science.ru.nl, R.Nolte@science.tu.nl, A.Rowan@science.ru.nl

Abstract

A ruthenium porphyrin functionalized with a cavity based on diphenylglycoluril is applied as a catalyst in carbenoid transfer reactions using α -diazoesters as substrates. The latter compounds contain a blocking group connected via an α,ω -dioxyalkyl spacer of 3 or 6 carbon atoms. The reaction of an excess of the α -diazoester with the short spacer with the ruthenium porphyrin macrocycle leads to two products, a [2]rotaxane and a maleate ester, which are the result of dimerization reactions at the inside and the outside of the cavity, respectively. A similar reaction using the α -diazoester with the long spacer also yields high molecular weight species. Mass spectrometric and NMR studies suggest that C-H and/or C=C insertion reactions take place on the thread of the initially formed rotaxane. It is proposed that these reactions are favoured by effective molarity effects because of the close proximity of reactive species in the interlocked geometry.

Keywords: rotaxanes; host-guest chemistry; ruthenium; porphyrins; carbenes; C-H insertion

Introduction

Rotaxanes are important members of the family of supramolecular architectures.¹ They consist of a dumbbell-shaped molecule, which is threaded through a macrocycle. These interlocked structures have been used as models for processive enzymes in nature² and have been applied³ as components of mechanical,⁴ (nano)electronic⁵ and electrochemical⁶ devices, sensors,⁷ and catalysts.^{2,8} There are a number of synthetic strategies by which rotaxanes can be prepared. Initially, statistical methods were used, but these were later largely replaced by methods based on a templated synthesis. Also an auto-catalytic threading approach has been reported.⁹ An alternative method to synthesize a rotaxane is to incorporate a metal center into its macrocyclic component and bind the two ‘half-thread’ dumbbell components,¹⁰ which are subsequently connected via a catalytic reaction mediated by the metal center. Following this approach, Cu(I)-functionalized macrocycles have for example been employed to catalyze the formation of a triazole linker between azido and alkyne-functionalized half-threads,¹¹ and Pd(II)-functionalized macrocycles for the oxidative coupling of terminal alkynes.¹² These approaches have in common that a large effective molarity of the reagents is realized, leading to a more efficient synthesis. Enzymes in nature operate in a similar way: they possess a binding pocket that binds the substrate and reactants in close proximity, thereby creating a high effective molarity resulting in a high reaction rate and a very selective reaction.

In this paper we employ the catalytically active ruthenium-porphyrin-functionalized macrocycle **Ru1** (Chart 1) to synthesize rotaxanes via a carbenoid transfer reaction. Subsequently, we make use of effective molarity effects to post-functionalize the rotaxane thread via additional carbene insertions (C=C and C-H), catalyzed by the same ruthenium porphyrin. Porphyrin macrocycles have been extensively studied in our group. In particular the Mn(III) analogue of **Ru1** is catalytically active in the epoxidation of alkenes.¹³ It also efficiently epoxidizes polymeric alkenes,^{2b,c} in a processive fashion^{2a} in which the catalytic macrocycle threads the substrate¹⁴ and remains bound to it during multiple catalytic turnovers. Because of its more extensive catalytic scope and versatility, we chose to use ruthenium as the metal center in the porphyrin macrocycle. In addition to oxidation reactions, ruthenium porphyrins can catalyze a wide variety of carbon-carbon couplings.¹⁵ Che and co-workers

reviewed carbenoid transfer reactions catalyzed by ruthenium porphyrins,¹⁶ such as cyclopropanations,¹⁷ carbon-hydrogen,¹⁸ nitrogen-hydrogen¹⁹ and sulphur-hydrogen²⁰ insertion reactions, 1,3-dipolar cycloadditions,²¹ olefination of aldehydes²² and dimerization reactions of diazo compounds.²³ We reasoned that the last reaction type would be of interest for the construction of rotaxanes, employing **Ru1** (Chart 1) as the catalyst. We selected the dimerization of α -diazoesters as the reaction to generate the rotaxane thread, yielding a maleate or fumarate ester depending on the stereochemical outcome of the double bond formation. The coupling has been proposed to occur via a ruthenium-carbene intermediate, which is formed after dissociation of an N_2 molecule from the α -diazoester.²³ The thread of the rotaxane subsequently offers a variety of options for post-modification using the same ruthenium porphyrin catalyst, e.g. oxidation or cyclopropanation of the olefin, or a C-H insertion reaction.

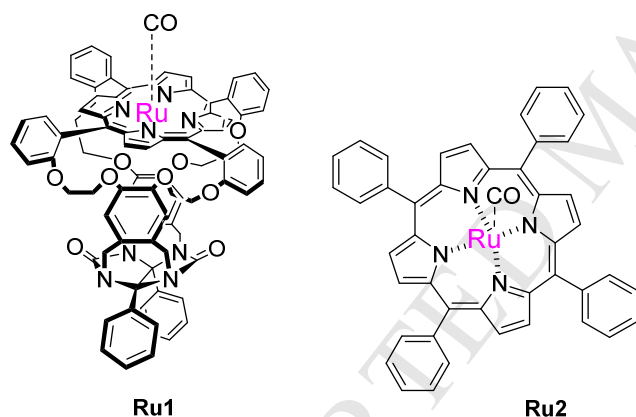
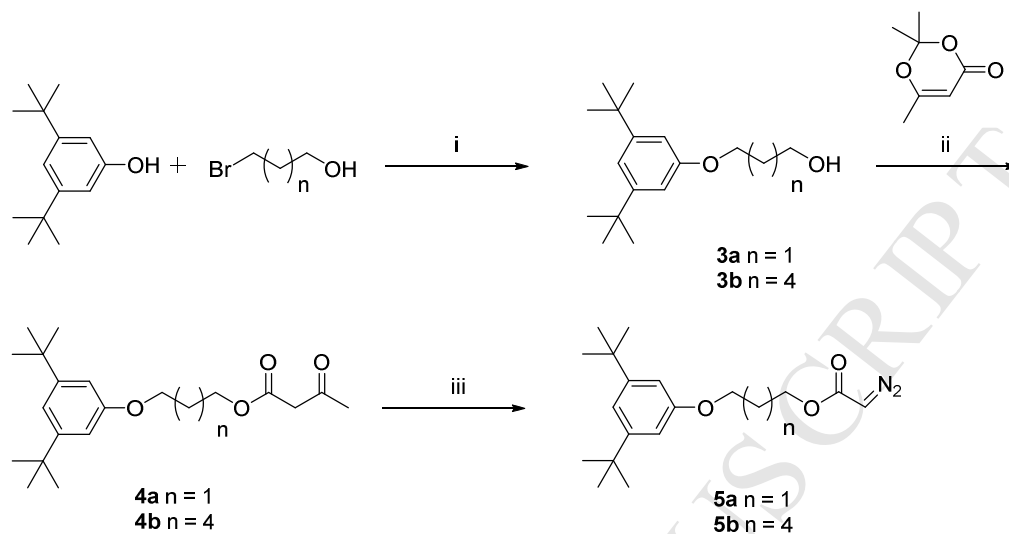


Chart 1: Structure of the catalytic ruthenium porphyrin macrocycle **Ru1**, and of reference complex **Ru2**.

Results and discussion

In order to be able to synthesize rotaxanes based on **Ru1** we first prepared the α -diazoesters **5a** and **5b** (Scheme 1). These compounds contain a bulky 3,5-di-*tert*-butylphenyl blocking group, coupled to the α -diazoester moiety via either a C-3 or a C-6 alkyl spacer, which is too large to fit in or slide through the cavity of the macrocycle. After alkylating 3,5-di-*tert*-butylphenol with the appropriate bromoalcohols, the resulting products **3a-b** were converted to β -diketoesters **4a-b** via a reaction with

2,2,6-trimethyl-4H-1,3-dioxin-4-one.²⁴ Subsequent reaction of compounds **4a-b** with 4-methylbenzenesulfonylazide^{23b} afforded α -diazooesters **5a-b**.



Scheme 1: Reagents and conditions: (i) K_2CO_3 , MeCN or DMF, ΔT , 16 h. (ii) toluene, reflux, 30 min. (iii) TsN_3 , Et_3N , MeCN, RT, 6 h, then LiOH, H_2O , RT, 16 h.

A ruthenium center was inserted into the free base porphyrin derivative of **Ru1**, **H₂1**^{13b,25} by a reaction with $\text{Ru}_3(\text{CO})_{12}$ in boiling phenol. Reference complex **Ru2** (Chart 1) was prepared using a literature procedure.²⁶ Slow evaporation of a chloroform solution of a 1:1 host-guest complex of **Ru1** and THF yielded crystals that were suitable for crystal structure analysis. The crystal structure revealed that an axially coordinated carbonyl ligand was located at the outside of the cavity of **Ru1** and a THF molecule inside the cavity (Figure 1).

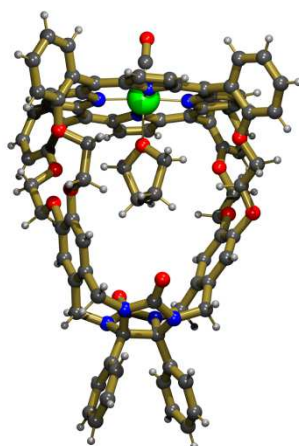
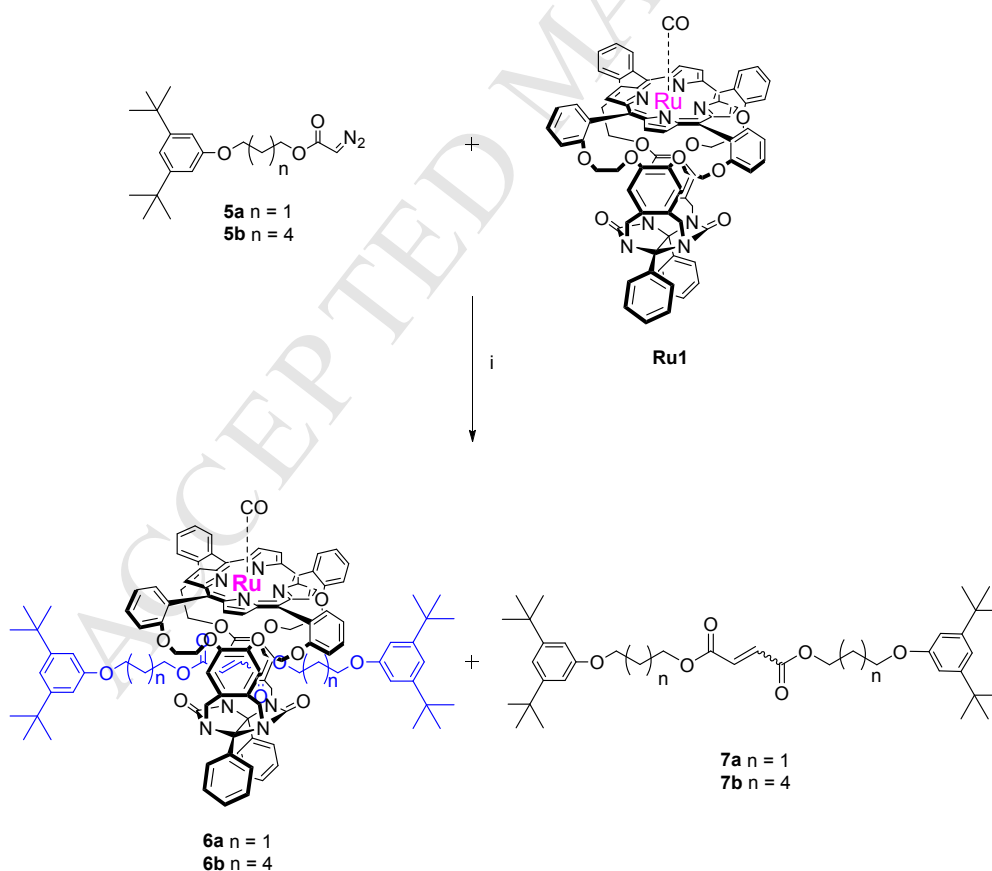


Figure 1: Crystal structure of **Ru1** with a THF guest molecule and a CO molecule coordinated to the ruthenium center.

The reaction of host **Ru1** with 2 equivalents of α -diazooesters (**5a** or **5b**) can, in principle, lead to two types of products (Scheme 2). When the reaction takes place at the “outside” of the cavity, homodimers **7a-b** will be generated, whereas rotaxanes **6a-b** can be expected as the products when the reaction takes places “inside” the cavity. In an initial experiment, two equivalents of **5a** were reacted with **Ru1** in 1,2-dichloroethane. The only new product formed was **7a**, which indicates that the coupling reaction had occurred exclusively on the outside of the macrocycle. Apparently, there is no favorable interaction between the highly polarized α -diazooester moiety and the polar crown ether and carbonyl groups of **Ru1**. When, however, the same reaction was carried out in the presence of a large excess (50 equiv.) of **5a**, the coupling reaction also occurred at the inside of the cavity, resulting in the formation of a mixture of rotaxane **6a** and compound **7a** (which was obtained exclusively as the (Z)-isomer, i.e., the maleate ester). After purification by column chromatography and preparative TLC, the rotaxane was obtained in 50% yield (based on the amount of **Ru1** used).



Scheme 2: Synthesis of rotaxanes **6a** and **6b**, and compounds **7a** and **7b**. Reagents and conditions: (i) 1,2-Dichloroethane, RT, 2.5 h.

^1H and ^{13}C NMR, MALDI-ToF and Accu-ToF spectra confirmed the identity of the formed rotaxane. In the ^1H -NMR spectrum of **6a** in CDCl_3 (Figure 2), proton signals H_d , H_e and H_f were shifted upfield by -1.12 , -1.69 and -1.67 ppm, respectively, compared to these signals in **7a**, as a result of the magnetic anisotropic shielding of the porphyrin moiety. The olefinic proton signal H_g of the maleate/fumarate functionality of the thread could not readily be identified in the spectrum. Since the double bond is most likely placed exactly underneath the porphyrin, a large upfield shift of its proton resonance is expected. With the help of ^{13}C - ^1H correlation NMR spectroscopy (HSQC) the alkene carbon signal at 125.5 ppm in the ^{13}C NMR spectrum was found to correlate with a very broad signal in the ^1H NMR spectrum located at 3.18 ppm. Compared to the same alkene C-H signal in **7a** (6.25 ppm), an upfield shift of -3.07 ppm has occurred. It was impossible to conclude from the broad NMR signals whether a fumarate ester, a maleate ester, or a mixture of both had been formed as the rotaxane thread. Additional evidence for a rotaxane geometry came from a 2D ROESY spectrum (see SI), in which nOe contacts were observed between blocking group proton H_b of the thread and β -pyrrole proton H_{12} of **Ru1**. Molecular modeling of **6a** indeed revealed that its blocking groups are positioned very close to the cavity portals and the porphyrin plane, due to the relatively short length of the thread, (Figure 3A).

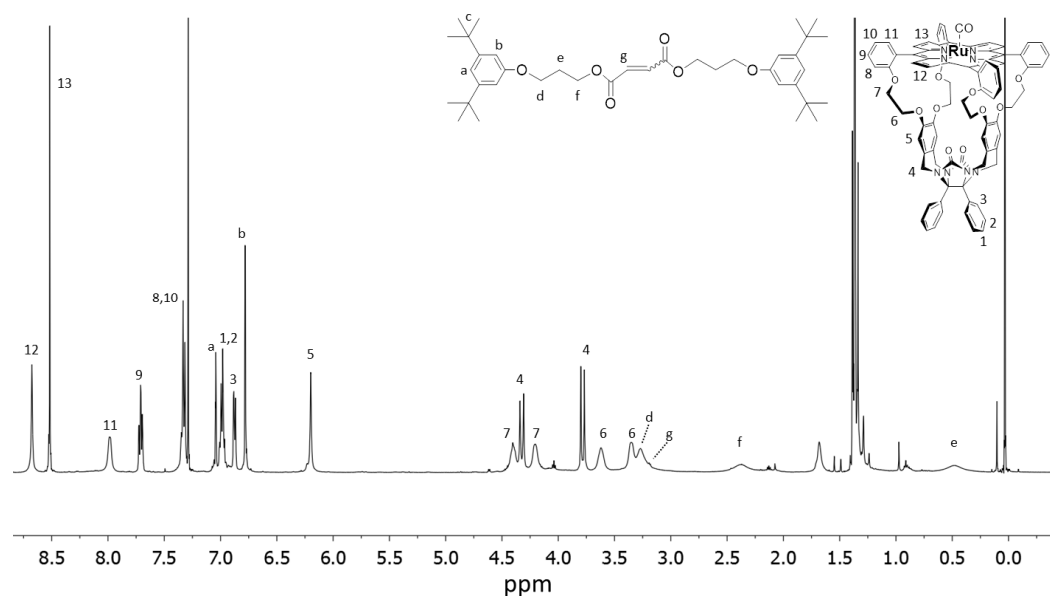


Figure 2 ^1H NMR spectrum (500 MHz, CDCl_3) and proton assignments of rotaxane **6a** (macrocycle and thread are drawn separately for clarity reasons).

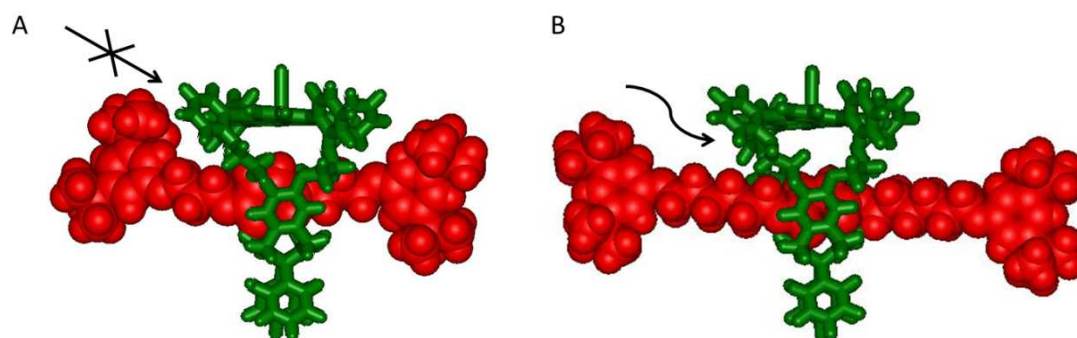


Figure 3 Molecular models of rotaxanes **6a** (A) and **6b** (B), showing the difference in accessibility of the cavity of the ruthenium porphyrin macrocycle for additional incoming α -diazoesters. The ruthenium-porphyrin macrocycle is represented as green sticks, the maleate/fumarate thread as red space-filling.

When aiming at subsequent post-modification of the thread using the ruthenium center of the rotaxane, this close proximity of the blocking groups to the cavity may hinder access of reagents, e.g., additional α -diazoesters. To overcome this restriction we decided to construct a rotaxane with a longer thread, **6b**, using an α -diazoester with a C-6 alkyl spacer (**5b**). Molecular modeling of **6b** (Figure 3B) revealed less blocking of the cavity and a considerable increase in the ability of the thread to move within the macrocycle. After employing the same protocol (the addition of 50 equiv. of α -diazoester to **Ru1**) as for the synthesis of rotaxane **6a**, TLC analysis of the crude product mixture showed several spots with the typical orange/red colour of a ruthenium porphyrin complex. The coupling of the α -diazoesters can in principle lead to the formation of rotaxanes with two isomeric threads, i.e., a maleate or a fumarate ester, but during the synthesis of rotaxane **6a** this did not give rise to multiple spots on TLC. Other porphyrin-containing reaction products could be an intermediate ruthenium-carbene species, or reaction products of additional α -diazoesters with the rotaxane. MALDI-ToF analysis (in linear mode, Figure 4) of the crude product showed a broad peak at 1790 amu, which probably corresponds to an intermediate Ru-porphyrin carbene species **8b** (Figure 5). Furthermore, a broad peak close to the expected mass of rotaxane **6b** (2164 amu) is observed, and a series of broad peaks, at quite regular mass intervals, corresponding to unexpected high molecular weight compounds. Roughly, these peaks can be identified with products with masses of the rotaxane + ($n \times 346$) amu ($n = 1,2,3,4$). A mass of 346 corresponds with the carbene that forms when α -diazoester **5b** loses a nitrogen

molecule in a reaction catalyzed by the ruthenium porphyrin. Such a carbene might subsequently be inserted into the double bond of the rotaxane thread, yielding a cyclopropane-like product with a mass of ($M_{6b} + 346$) amu. However, such a cyclopropanation can only occur once, leaving the products with higher molecular masses unexplained. Other possibilities are that additional carbene fragments react with the rotaxane thread via insertion reactions into one of the C-O-C=O, Ar-O-CH₂-, or alkyl C-H bonds, or attach to the framework of the macrocyclic host. The latter possibility is discarded since during the reaction of **Ru1** with **5a** no reactions with the framework of the host were observed.

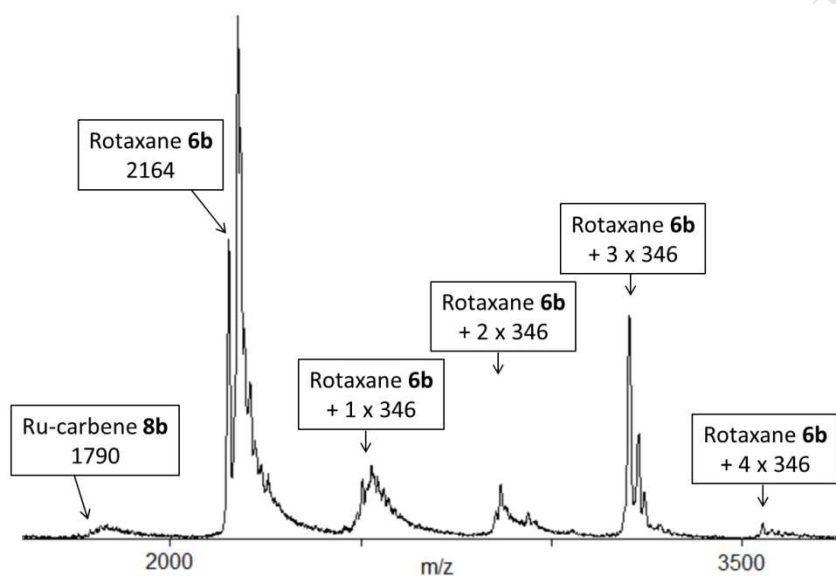


Figure 4: MALDI-ToF spectrum (linear mode) showing high molecular weight compounds after the reaction of an excess of **5b** with **Ru1**.

After column chromatography, rotaxane **6b** could be isolated in 41% yield. The remaining orange/red material (characterized by the high molecular weight peaks in the MALDI-ToF spectrum) always eluted as a single fraction, both on silica columns as on a size-exclusion column. We can therefore not unambiguously determine whether this material consists of a single product that fragments during the MALDI-ToF measurement, or represents a product distribution. Both materials were analyzed with the help of NMR spectroscopy (Figure 6). The ¹H NMR spectrum of **6b** (Figure 6A) resembles that of rotaxane **6a**. The inclusion of the thread inside the cavity of **Ru1** can again be concluded from the observed upfield shifts of in particular protons H_g-H_j, as a result of shielding by the porphyrin ring current. Although the NMR spectrum of the high molecular weight material (Figure 6B) still shows

many of the characteristics of a rotaxane-like species, it is strikingly different and very complex compared to the spectrum of **6b**. Particularly remarkable is the presence of a series of substantial, broad proton signals between +1 and -1 ppm.

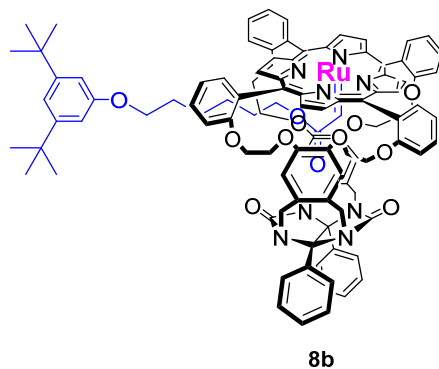


Figure 5 Structure of the expected intermediate ruthenium-carbene species **8b** during the reaction between **Ru1** and **5b**.

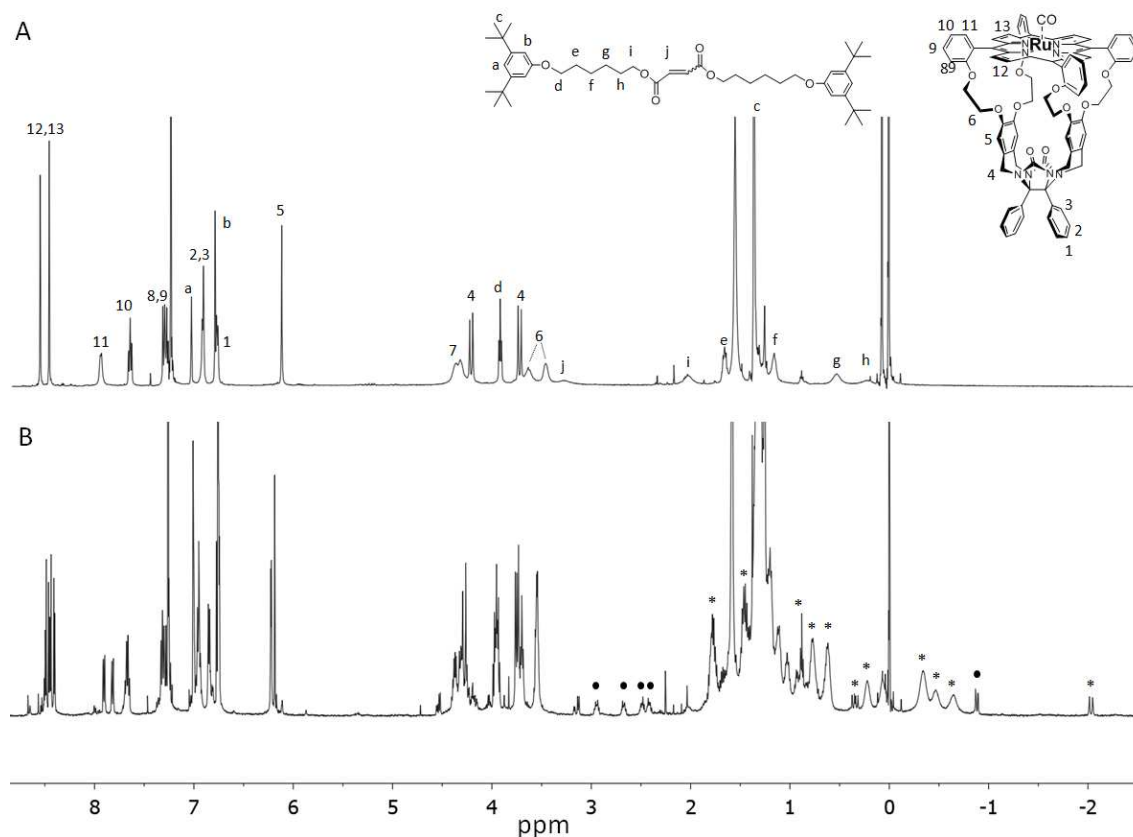
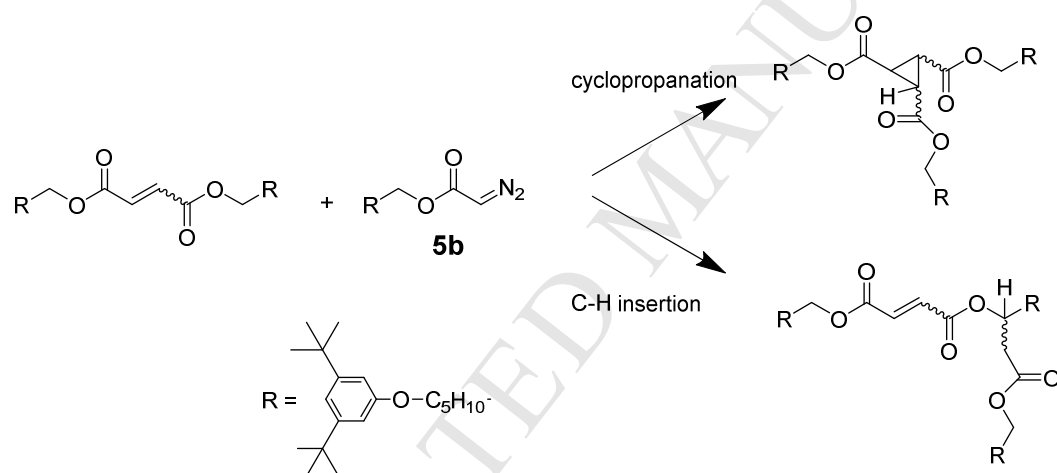


Figure 6 ^1H NMR spectra (500 MHz, CDCl_3) of (A) rotaxane **6b** including assignment of the protons of the macrocyclic host and the thread (macrocycle and thread are drawn separately for clarity reasons), and (B) the product containing the high molecular masses; the signals indicated with (*) all correlate with ^{13}C -signals between 25 and 30 ppm, and the signals indicated with (•) all correlate with ^{13}C -signals between 62 and 64 ppm (see text for explanation).

Interestingly, when similar coupling reactions of **5a** or **5b** were carried out using a reference ruthenium porphyrin such as **Ru2** (Chart 1) as the catalyst, exclusively the maleate isomers of **7a** and **7b** were formed, and no higher molecular weight compounds. This indicates that the presence of the receptor cavity of **Ru1** is essential for the formation of such compounds. Several possibilities for the difference in catalytic behavior of **Ru1** compared to a ruthenium porphyrin without a cavity can be envisaged: (i) the crown-ether spacers and the carbonyl oxygen atoms of the cavity may create a polar environment that interacts favourably with α -diazoester substrates, increasing their affinity for the cavity; this option is, however, not likely since an excess of α -diazoester was found to be required for a preferred coupling reaction *inside* the cavity; (ii) as a result of ring tension due to the attachment of a rigid cavity, the porphyrin may experience a doming effect, changing its reactivity; this possibility is also unlikely since the X-ray structure of **Ru1** revealed that its porphyrin roof is almost perfectly planar; (iii) an *effective molarity* effect: once rotaxane **6b** has been formed, the effective molarity of the thread component inside the cavity of **Ru1** is much higher than it would be in the case when it can diffuse away after the coupling reaction (for example, when such a reaction occurs at the outside of the cavity, or when it is catalyzed by **Ru2**). Therefore, as a result of the interlocked nature of the complex, the thread of **6b** will always reside in very close proximity to the catalytic Ru-center in potential follow-up reactions. We propose that this effective molarity effect is responsible for the observed reaction(s) of the thread with additional incoming α -diazoesters.

The complexity of the MALDI-ToF and NMR spectra of the high molecular mass material makes its identification and the elucidating of its formation mechanism very challenging. A combination of NMR techniques was used to get an insight in the structure of the formed product(s). In the ^1H NMR spectrum (Figure 6B) many signals of the macrocyclic host are split and/or doubled, indicating a non-symmetric complexation of a guest in the cavity. ^{13}C - ^1H correlation spectra (see SI) revealed that the series of broad signals between 2 and -1 ppm (indicated by (*)) in the NMR spectrum) can be assigned to $-\text{CH}_2\text{CH}_2\text{CH}_2-$ protons, since they all correlate with ^{13}C signals between 25 and 30 ppm. These protons must arise from the spacer of a thread component. The sharp signals at 0.34 and -2.03 ppm, correlate with ^{13}C signals at 23 ppm, which are quite typical for the presence of a cyclopropane ring

structure. Compared to the ^1H NMR spectrum of **6b**, also a series of new, relatively sharp signals was found between 3.0 and 2.3 ppm, and at -0.88 ppm (indicated by \bullet in the NMR spectrum), that all correlate with ^{13}C signals between 62 and 64 ppm. These signals are assigned to $-\text{CH}_2\text{OC}(\text{O})-$ or $-\text{CHOC}(\text{O})-$ protons, that also must come from a thread component. Remarkably, according to a HSQC spectrum (signal at 62 ppm), the signal at -0.88 ppm appears to correspond to a $-\text{CH}(\text{R})-\text{OC}(\text{O})-$ proton. This is a key observation with regard to elucidating the reaction mechanism, since such protons are not present in a linear coupling product such as **7b**. We therefore propose that a thread component must be present in which α -diazoester **5b** has inserted into either the double bond of the alkene of a preformed linear thread (C=C insertion), or into an alkyl spacer (C-H insertion), or into both (Scheme 3).



Scheme 3 Examples of possible reactions of the thread of rotaxane **6b** with α -diazoester **5b**.

While a cyclopropanation can occur only once, multiple C-H insertion reactions may take place, which would explain the masses in the MALDI-ToF spectrum of $M_{6b} + (n \times 346)$ amu ($n = 1,2,3,4$). Apparently, after 4 insertion reactions no more additional α -diazoesters are attached, which can be envisaged when the progressive increase in steric crowding of the rotaxane thread after each insertion is considered. A branched thread is formed, which eventually will lose all its mobility with respect to the macrocyclic host, and will block access to the cavity for additional insertions. An example of such a branched rotaxane product is depicted in Figure 7.

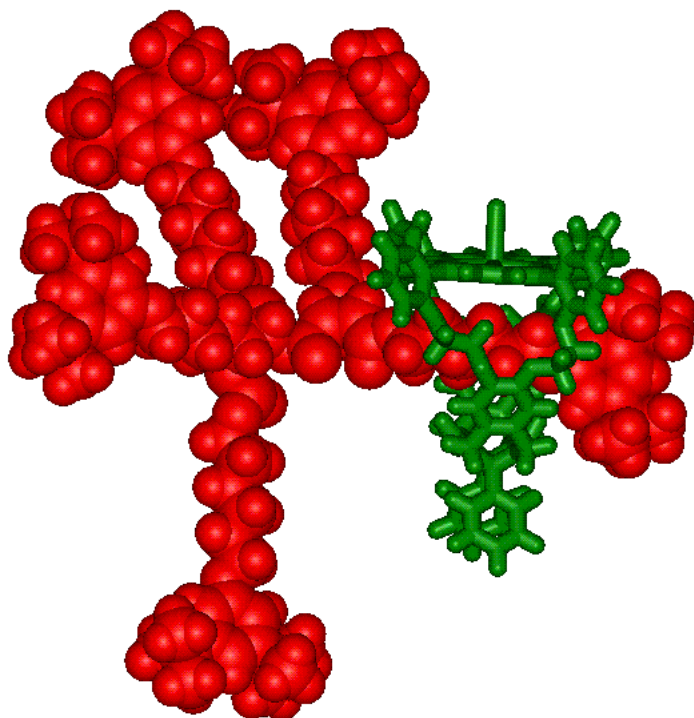


Figure 7 Proposed possible structure of a high molecular mass product in which three carbenes formed from α -diazoester **5b** have inserted into the thread of rotaxane **6b**: one in the C=C bond forming a cyclopropane, and two into the CH₂-groups next to the ester. The ruthenium-porphyrin macrocycle is represented as green sticks, the branched thread as red space-filling.

Conclusion

We have demonstrated that a ruthenium porphyrin-functionalized macrocycle based on diphenylglycoluril can serve as carbenoid transfer catalyst for the dimerization of α -diazoesters inside its cavity. When these α -diazoesters contain bulky blocking groups, rotaxanes are formed. A short alkyl spacer (C-3) between the α -diazoester moiety and the blocking group yields a rotaxane with exclusively a linear thread composed of two carbene moieties. When a longer spacer (C-6) is used, additional reactions of the α -diazoester with the rotaxane yield higher molecular mass products, in which up to 4 extra carbenes are incorporated into the rotaxane thread. NMR and mass spectrometric studies indicate that these reactions involve C=C and C-H insertions. The observation that a reference ruthenium porphyrin without a cavity does not display such post-modification abilities is attributed to an effective molarity effect exhibited by the rotaxane: once this interlocked species is formed, the effective molarity of the thread inside the ruthenium-porphyrin macrocycle is so high that additional reactions with α -diazoesters readily take place, because of their close proximity to the catalytic metal center. The observation that the rotaxane with short C-3 alkyl spacers is inert towards such insertion reactions is attributed to the restricted access of additional α -diazoesters to its cavity, due to the close proximity of the blocking groups.

Experimental

Methods and materials

Solvents used for synthesis were dried using standard procedures and freshly distilled before use. Other chemicals were used as received. 1D and 2D ^1H and ^{13}C NMR spectra were recorded on a FDRX-500 instrument. Chemical shifts (δ) are reported in ppm downfield from the internal standard TMS (0.00 ppm). Abbreviations used are: s = singlet, d = doublet, t = triplet, q = quartet, m = multiplet, br = broad. LCQ mass spectra were recorded on a Thermo Finnigan LCQ Advantage Max spectrometer. Accurate mass spectra were recorded on a JEOL AccuTOF CS JMS-T100CS instrument. MALDI-ToF mass spectra were recorded on Bruker Biflex III and Bruker Microflex LRF instruments, using dithranol as the matrix. FT-IR spectra were recorded on a Bruker Tensor-27 machine, and UV-vis spectra on a Varian Cary-50 UV-VIS spectrophotometer. For column chromatography Silica (0.063-0.200 mm) from J.T. Baker was used, and for size exclusion chromatography Bio-Beads SX1, 200-400 mesh, from Bio-Rad.

Syntheses

Ruthenium porphyrin macrocycle Ru1: Compound **H₂1**^{13a,25} (55 mg, 0.041 mmol), tris-rutheniumdodecacarbonyl (Ru₃(CO)₁₂) (79 mg, 0.124 mmol), and phenol (500 mg) were placed under an argon atmosphere in a 10 mL Schlenk flask. The reaction mixture was heated in a 190 °C sand-bath and stirred for 45 minutes. The mixture was cooled to room temperature and directly purified by silica column chromatography using a polarity gradient. Unreacted Ru₃(CO)₁₂ was removed by elution with pure dichloromethane (yellow/orange band), and phenol with a dichloromethane/methanol mixture (99.9/0.1 v/v). Finally, the product was obtained by eluting with a more polar mixture of dichloromethane/methanol (9.9/0.1 v/v). The product was dissolved in a minimum amount of dichloromethane and precipitated by adding 10 mL of *n*-heptane. The dichloromethane was removed under vacuum and the product was isolated from the *n*-heptane layer by centrifugation at 2000 rpm. It was dried *in vacuo*. Yield: 54 mg (0.037 mmol, 91%) of **Ru1** as a bright red solid. Single crystals suitable for X-ray diffraction were obtained from slow evaporation of a CDCl₃/THF (999:1, v/v) solution of the compound. ¹H NMR (500 MHz, CDCl₃): δ 8.68 (s, 4H, β-pyrroleH), 8.60 (s, 4H, β-pyrroleH), 8.12 (d, *J* = 7.0 Hz, 4H, ArH), 7.73 (t, *J* = 7.9 Hz, 4H, ArH), 7.40 (t, *J* = 7.4 Hz, 4H, ArH), 7.33 (d, *J* = 8.3 Hz, 4H, ArH), 6.96 (m, 6H, ArH), 6.83 (m, 4H, ArH), 6.19 (s, 4H, ArH), 4.21 (d, *J* = 15.8 Hz, 4H, NCH₂Ar), 4.13 (m, 4H, CH₂O), 3.94 (m, 4H, CH₂O), 3.73 (d, *J* = 15.7 Hz, 4H, NCH₂Ar), 3.51 (m, 4H, CH₂), 3.28 (m, 4H, CH₂O). ¹³C NMR (125 MHz, CDCl₃): δ 158.92, 157.34, 146.62, 144.43, 144.01, 135.76, 133.95, 132.76, 131.76, 129.50, 128.80, 128.62, 128.16, 120.62, 117.22, 116.08, 113.84, 85.08, 68.15, 44.35, 35.57, 32.03, 29.17, 26.59, 22.84, 14.27. Accurate mass (Accu-ToF): 1527.37414 (**Ru1** + MeOH + Na⁺) (mass difference 2.55 ppm). Diffusion coefficient (DOSY) 5.95 * 10⁻¹⁰ m²/s. UV-vis (CHCl₃): 413, 527 nm.

5,10,15,20-Tetraphenylporphyrinato ruthenium carbonyl (Ru2): This compound was prepared according to a literature procedure.²⁶

3-(3,5-Di-*tert*-butylphenoxy) propan-1-ol (3a): A 250 mL Schlenk round bottom flask was charged with 3,5-di-*tert*-butylphenol (2.70 g, 13.09 mmol), 3-bromopropan-1-ol (1.66 g, 11.96 mmol), K₂CO₃ (1.83 g, 13.23 mmol), and 45 mL of argon-purged acetonitrile. The mixture was placed under an argon atmosphere and refluxed for 16 h. The suspension was cooled to room temperature and the salts were filtered off. The solution was concentrated *in vacuo* and the solid crude product was purified by silica chromatography (eluent ethyl acetate/*n*-heptane 1:3 v/v). Compound **3a** was obtained as a colorless oil (2.78 g, 10.52 mmol, yield 88%). ¹H NMR (500 MHz, CDCl₃): δ 7.04 (t, *J* = 1.6 Hz, 1H, *p*-ArH), 6.78 (d, *J* = 1.6 Hz, 2H *o*-ArH), 4.15 (t, *J* = 5.9 Hz, 2H, Ar-O-CH₂), 3.89 (q, *J* = 5.7 Hz, 2 H, CH₂-OH), 2.06 (qn, *J* = 5.9 Hz, 2H, O-CH₂-CH₂-CH₂-OH), 1.93 (t, *J* = 5 Hz, 1H, OH), 1.32 (s, 18 H, CH₃). ¹³C NMR (125 MHz, CDCl₃): δ 158.44, 152.40, 115.33, 108.95, 65.95, 61.00, 35.13, 32.26, 31.58. Mass (LCQ): 551 (2M + Na⁺).

3-(3,5-Di-*tert*-butylphenoxy) hexan-1-ol (3b): A 250 mL Schlenk round bottom flask was charged with 3,5-di-*tert*-butylphenol (1.14 g, 5.56 mmol), 3-bromohexan-1-ol (1.0 g, 5.56 mmol), K₂CO₃ (3.0 g, 21.7 mmol), and 30 mL of argon-purged DMF. The mixture was placed under an argon atmosphere and heated at 100°C for 16 h. The suspension was cooled to room temperature and the salts were filtered off. The solution was concentrated *in vacuo* and the solid crude product was purified by silica chromatography (eluent ethyl acetate/*n*-heptane 1:4 v/v). Compound **3b** was obtained as a pale yellow oil (1.21 g, 3.99 mmol, yield 71%). ¹H NMR (500 MHz, CDCl₃): δ 7.05 (t, *J* = 1.5 Hz, 1H, *p*-ArH), 6.79 (d, *J* = 1.5 Hz, 2H *o*-ArH), 4.17 (t, *J* = 6.0 Hz, 2H, Ar-O-CH₂), 3.90 (q, *J* = 5.9 Hz, 2 H, CH₂-OH), 1.8-1.45 (m, 8H, CH₂), 1.95 (br, 1H, OH), 1.31 (s, 18 H, CH₃). ¹³C NMR (125 MHz, CDCl₃): δ 158.63, 152.13, 114.83, 108.81, 67.58, 62.93, 34.98, 32.72, 31.45, 29.47, 25.99, 25.59. Mass (MALDI-ToF): 307 ([M + H]⁺).

3-(3,5-Di-*tert*-butylphenoxy)propyl-3-oxobutanoate (4a): Compound **3a** (2.27 g, 8.59 mmol) was dissolved in 15 mL of toluene and placed in a three-necked roundbottom flask equipped with an addition funnel and a distillation setup. The mixture was placed under argon and heated to 110 °C after which 2,2,6-trimethyl-4H-1,3-dioxin-4-one (1.34 g, 9.44 mmol) in 6 mL of toluene was added dropwise. The formed acetone was removed by applying a small stream of argon. The mixture was stirred at 100 °C for 30 min. The solvent was removed and the crude product was purified by silica chromatography (eluent ethyl acetate/*n*-heptane 1:3 v/v). Compound **4a** was obtained as a yellowish oil in a yield of 72% (2.16 g, 6.19 mmol). ¹H NMR (500 MHz, CDCl₃) δ 12.08 (s, COH enol), 7.02 (t, *J* = 1.5 Hz, 1H, *p*-ArH), 6.68 (d, *J* = 1.5 Hz, 2H, *o*-ArH), 4.98 (s, CH enol), 4.38 (t, *J* = 6.4 Hz, 2H, Ar-O-CH₂), 4.35 (s, 2H, Ar-O-CH₂ enol), 4.07 (t, *J* = 6.1 Hz, 2H, CH₂-O-C=O), 3.47 (s, 2H, O=C-CH₂-C=O), 2.27 (s, 3H, O=C-CH₃), 2.16 (q, *J* = 6.2 Hz, 2H, CH₂-CH₂-CH₂), 1.96 (t, *J* = 0.6 Hz, -C(OH)CH₃ enol), 1.32 (s, 18 H *t*-butyl). ¹³C NMR (125 MHz, CDCl₃): δ 200.52, 175.74, 167.21, 158.40, 152.37, 115.28, 108.93, 89.80, 64.17, 63.99, 62.51, 61.03, 50.17, 35.11, 31.57, 30.27, 28.98, 28.79, 21.33). Mass (LCQ): 719 ([2M + Na]⁺).

3-(3,5-Di-*tert*-butylphenoxy)hexyl-6-oxobutanoate (4b): Compound **3b** (0.975 g, 3.19 mmol) was dissolved in 10 mL of toluene and placed in a three-necked roundbottom flask equipped with an addition funnel and a distillation setup. The mixture was placed under argon and heated to 110 °C after which 2,2,6-trimethyl-4H-1,3-dioxin-4-one (0.496 g, 3.49 mmol) in 4 mL of toluene was added dropwise. The formed acetone was removed by applying a small stream of argon. The mixture was stirred at 100 °C for 1 h. The solvent was removed and the crude product was purified by silica chromatography (eluent ethyl acetate/*n*-heptane 1:7 v/v). Compound **4b** was obtained as a colourless oil in a yield of 83% (1.03 g, 2.64 mmol). ¹H NMR (500 MHz, CDCl₃): δ 12.07 (s, COH enol), 7.04 (t, *J* = 1.6 Hz, 1H, *p*-ArH), 6.67 (d, *J* = 1.6 Hz, 2H, *o*-ArH), 5.01 (d, *J* = 0.7 Hz, CH enol), 4.18 (t, *J* = 6.3 Hz, 2H, Ar-O-CH₂), 3.85 (t, *J* = 6.1 Hz, 2H, CH₂-O-C=O), 3.43 (s, 2H, O=C-CH₂-C=O), 2.28 (s, 3H, O=C-CH₃), 1.82-1.41 (m, 8H, -CH₂-), 1.31 (s, 18H, *t*-butyl). Mass (LCQ): 391 ([M + H]⁺).

3-(3,5-Di-*tert*-butylphenoxy)propyl 2-diazoacetate (5a): Compound **4a** (2.15 g, 6.17 mmol) was dissolved in a mixture of acetonitrile (8 mL) and triethylamine (1.02 mL, 6.72 mmol). A solution of 4-methylbenzenesulfonyl azide^{23b} (1.75 g, 8.88 mmol) in 8 mL of acetonitrile was added slowly (± 10 min). The mixture was stirred at room temperature for 6 hrs. Thereafter, an aqueous solution of lithium hydroxide hydrate (1.00 g, 23.88 mmol) was added and the reaction was stirred overnight. The product was extracted with diethyl ether (4×35 mL), and the combined ether layers were washed with brine (2 \times) and dried over Na₂SO₄. The solvent was removed *in vacuo* and the product was purified by column chromatography with ethyl acetate/*n*-heptane (2:8 v/v) as the eluent. Compound **5a** was obtained as a yellow oil (1.75 g, 5.25 mmol, 85 % yield). ¹H NMR (500 MHz, CDCl₃): δ 7.04 (t, $J = 1.6$ Hz, 1H, *p*-ArH), 6.76 (d, $J = 1.6$ Hz, 2H, *o*-ArH), 4.76 (br s, 1H, CH=N₂), 4.39 (t, $J = 6.3$ Hz, 2H, Ar-O-CH₂), 4.06 (t, $J = 6.1$ Hz, 2H, CH₂-O-C=O), 2.14 (p, $J = 6.2$ Hz, 2H, CH₂-CH₂-CH₂), 1.32 (s, 18H, CH₃). ¹³C NMR (125 MHz, CDCl₃): δ 158.44, 152.37, 115.27, 108.95, 64.10, 62.01, 46.35, 35.12, 31.58, 29.12. Mass (LCQ): 687 (2M + Na⁺). (MALDI-ToF): 333 ([M + H]⁺). IR (KBr pellet) 2109 cm⁻¹ (C=N₂).

3-(3,5-Di-*tert*-butylphenoxy)hexyl 2-diazoacetate (5b): Compound **4b** (1.0 g, 2.56 mmol) was dissolved in a mixture of acetonitrile (5 mL) and triethylamine (0.5 mL). A solution of 4-methylbenzenesulfonyl azide^{23b} (0.722 g, 3.67 mmol) in 5 mL of acetonitrile was added slowly (± 10 min). The mixture was stirred at room temperature for 6 h. Thereafter, an aqueous solution of lithium hydroxide hydrate (0.45 g, 11.8 mmol) was added and the reaction was stirred overnight. The product was extracted with diethyl ether (2×25 mL), and the combined ether layers were washed with brine ($2\times$) and dried over Na_2SO_4 . The solvent was removed *in vacuo* and the product was purified by column chromatography with CHCl_3 as the eluent. Compound **5b** was obtained as a yellow oil that solidified upon standing (0.762 g, 2.03 mmol, 79% yield). ^1H NMR (500 MHz, CDCl_3): δ 7.01 (t, $J = 1.5$ Hz, 1H, *p*-ArH), 6.75 (d, $J = 1.5$ Hz, 2H, *o*-ArH), 4.73 (br s, 1H, $\text{CH}=\text{N}_2$), 4.18 (t, $J = 6.2$ Hz, 2H, Ar-O- CH_2), 3.96 (t, $J = 6.1$ Hz, 2H, $\text{CH}_2\text{-O-C=O}$), 1.79 (m, 2H, Ar-O- CH_2CH_2), 1.68 (m, 2H, Ar-O- $\text{CH}_2\text{CH}_2\text{CH}_2\text{CH}_2\text{CH}_2$), 1.53 (m, 2H, Ar-O- $\text{CH}_2\text{CH}_2\text{CH}_2$), 1.45 (m, 2H, Ar-O- $\text{CH}_2\text{CH}_2\text{CH}_2\text{CH}_2$), 1.31 (s, 18H, CH_3). ^{13}C NMR (125 MHz, CDCl_3): δ 166.93, 158.61, 152.15, 114.87, 108.79, 67.51, 65.14, 46.16, 34.99, 31.46, 29.39, 28.78, 25.84, 25.72. Mass (MALDI-ToF): 375 ($[\text{M} + \text{H}]^+$).

Rotaxane 6a: To a solution of **Ru1** (16 mg, 10.87 μmol) in 2.25 mL of 1,2-dichloroethane (distilled from CaH_2) was added compound **5a** (181 mg, 0.543 mmol) dissolved in 1.5 mL of 1,2-dichloroethane. The mixture was stirred for 2.5 hrs at room temperature under an argon atmosphere and then placed on a silica column. Using dichloromethane as the eluent, the formed homodimer **7a** was eluted first. Rotaxane **6a** was subsequently collected by using $\text{CH}_2\text{Cl}_2/\text{MeOH}$ 98:2 (v/v) as the eluent. Preparative TLC (eluent *n*-heptane/ethyl acetate 6:4 (v/v)) was applied to purify the rotaxane further. Yield: 10.5 mg, 5.04 μmol , 46%) of an orange/red solid. ^1H NMR (500 MHz, CDCl_3 , see Figure 2 for a detailed peak assignment): δ 8.65 (s, 4H, β -pyrroleH), 8.49 (s, 4H, β -pyrroleH), 7.96 (bs, 4H, ArH), 7.71 (t, 4H, $^3J = 8.0$ Hz, ArH), 7.31 (m, 8H, ArH), 7.02 (t, $^4J = 1.5$ Hz, 2H, ArH), 6.96 (m, 6H, ArH), 6.85 (m, 4H, ArH), 6.75 (d, 4H, $^4J = 1.6$ Hz, ArH), 6.17 (s, 4H, ArH), 4.38 (bs, 4H, $\text{CH}_2\text{-O}$), 4.30 (d, $^2J = 15.9$ Hz, 4H, NCH_2Ar), 4.18 (bs, 4H, $\text{CH}_2\text{-O}$), 3.76 (d, $^2J = 15.8$ Hz, 4H, NCH_2Ar), 3.59 (bs, 4H, $\text{CH}_2\text{-O}$), 3.33 (bs, 4H, $\text{CH}_2\text{-O}$), 3.27 (bs, 2H, Ar- OCH_2), 3.18 (br s, 2H, $\text{CH}=\text{CH}$), 2.37 (bs, 4H, $\text{CH}_2\text{-O}(\text{CO})$), 1.34 (s, 36H, CH_3), 0.48 (bs, 4H, $\text{CH}_2\text{CH}_2\text{CH}_2$). ^{13}C NMR (125 MHz, CDCl_3): δ 182.36, 158.57, 158.33, 158.24, 156.78, 152.18, 146.71, 146.57, 144.46, 143.80, 136.71, 134.13, 132.24, 131.55, 130.38, 129.92, 129.22, 128.55, 128.37, 119.83, 117.24, 114.88, 114.78, 111.31, 108.90, 108.62, 84.72, 77.16, 67.49, 66.70, 64.35, 62.02, 44.55, 35.15, 31.74, 31.58, 29.85, 27.44 Accurate mass (Accu-ToF, Na^+ -adduct): 2103.75561 (mass difference 4.28 ppm). Diffusion coefficient DOSY: $4.1 * 10^{-10}$. IR [KBr] 1935 cm^{-1} (CO). UV-Vis: 415, 532, 536 nm.

Rotaxane 6b: To a stirred, degassed solution of **Ru1** (10 mg, 6.79 μmol) in 1,2-dichloroethane (5 mL) was added a degassed solution of **5b** (127 mg, 0.340 mmol) in 1,2-dichloroethane (1.5 mL) in 3 portions over 5 min. The mixture was stirred under argon for 3 h. The crude product was first purified by column chromatography (silica, gradient $\text{CH}_2\text{Cl}_2 - \text{CH}_2\text{Cl}_2/\text{MeOH}$ 9:1, v/v) and then by size exclusion column chromatography (toluene). Two orange/red fractions were isolated, of which the second was rotaxane **6b** (yield: 6 mg, 41%). ^1H NMR (500 MHz, CDCl_3) δ ^1H NMR (ppm, see Figure 6A for a detailed peak assignment): δ 8.58 (s, 4H, β -pyrroleH), 8.49 (s, 4H, β -pyrroleH), 7.97 (d, 4H, $^3J = 6.7$ Hz, ArH), 7.67 (t, 4H, $^3J = 8.1$ Hz ArH), 7.35-7.21 (m, 8H, ArH), 7.05 (t, $^4J = 1.5$ Hz, 2H, ArH), 6.94 (m, 6H, ArH), 6.82-6.75 (m, 4H, ArH), 6.81 (d, 4H, $^4J = 1.6$ Hz, ArH), 6.14 (s, 4H, ArH), 4.35 (m, 8H, $\text{CH}_2\text{-O}$), 4.22 (d, $^2J = 15.9$ Hz, 4H, NCH_2Ar), 3.93 (t, $^3J = 6.5$ Hz, 4H, Ar-O- CH_2), 3.73 (d, $^2J = 15.9$ Hz, 4H, NCH_2Ar), 3.64 (m, 4H, $\text{CH}_2\text{-O}$), 3.47 (m, 4H, $\text{CH}_2\text{-O}$), 3.29 (br s, 2H, $\text{CH}=\text{CH}$), 2.02 (m, 4H, $\text{CH}_2\text{-O}(\text{CO})$), 1.66 (m, 4H, $-\text{CH}_2-$), 1.36 (s, 36H, CH_3), 1.57 (m, 4H, $-\text{CH}_2-$), 0.52 (br s, 4H, $-\text{CH}_2-$), 0.22 (br s, 4H, $-\text{CH}_2-$). Mass (MALDI-ToF): 2137 ($[\text{M} - \text{CO} + \text{H}]^+$), 2164 ($[\text{M}]^+$). IR [KBr] 1936 cm^{-1} (CO). UV-Vis: 415, 535 nm.

bis(3-(3,5-Di-tert-butylphenoxy)propyl) maleate (7a): This compound was obtained as a side-product during the synthesis of rotaxane **6a**. ^1H NMR (500 MHz, CDCl_3 , ppm): δ 7.02 (t, $^4J = 1.5$ Hz, 2H, Ar-H), 6.75 (d, $^4J = 1.5$ Hz, 4H, Ar-H), 6.25 (s, 2H, $\text{CH}=\text{CH}$), 4.39 (t, $^3J = 6.9$ Hz, 4H Ar-O CH_2), 4.06 (t, $^3J = 6.1$ Hz, 4H, $\text{CH}_2\text{-O}(\text{CO})$), 2.15 (p, $^3J = 6.2$ Hz, 4H, $\text{CH}_2\text{CH}_2\text{CH}_2$), 1.31 (s, 36H, CH_3) ppm. ^{13}C NMR (125 MHz, CDCl_3 , ppm): δ 165.3, 158.4, 152.3, 129.9, 115.2, 108.9, 64.0, 62.4, 35.1, 31.6, 28.7 ppm. Mass (MALDI-ToF): 609 ($[\text{M} + \text{H}]^+$).

bis(3-(3,5-Di-tert-butylphenoxy)hexyl) maleate (7b): This compound was obtained as a side-product during the synthesis of rotaxane **6b**. ^1H NMR (500 MHz, CDCl_3): δ 7.01 (br s, 2H, Ar-H), 6.75 (br s, 4H, Ar-H), 6.23 (s, 2H, $-\text{CH}=\text{CH}-$), 4.19 (t, $^3J = 6.9$ Hz, 4H, ArO- CH_2-), 3.95 (t, 4H, $-\text{CH}_2\text{-O}(\text{CO})-$), 1.79 (m, 4H, $-\text{CH}_2-$), 1.69 (m, 4H, $-\text{CH}_2-$), 1.52 (m, 4H, $-\text{CH}_2-$), 1.44 (m, 4H, $-\text{CH}_2-$), 1.33 (s, 18H, CH_3). Mass (MALDI-ToF): 693 ($[\text{M} + \text{H}]^+$).

Crystal structure of Ru1.THF Crystallographic data (excluding structure factors) for the structures in this paper have been deposited with the Cambridge Crystallographic Data Centre as supplementary publication no. CCDC 1542345. Copies of the data can be obtained, free of charge, on application to CCDC, 12 Union Road, Cambridge CB2 1EZ, UK, (fax: +44-(0)1223-336033 or e-mail: deposit@ccdc.cam.ac.uk).

Acknowledgements

This research was supported by NanoNed - the Dutch nanotechnology initiative by the Ministry of Economic Affairs. Further financial support was obtained from the European Research Council in the form of an ERC Advanced grant to R.J.M.N. (ALPROS-290886) and an ERC Starting grant to J.A.A.W.E (NANOCAT-259064), the Council for the Chemical Sciences of the Netherlands Organization for Scientific Research (CW-NWO) (Vidi grant for J.A.A.W.E and Vici grant for A.E.R), and from the Ministry of Education, Culture, and Science (Gravity program 024.001.035).

References

1. (a) Balzani V, Gomez-Lopez M, Stoddart JF. *Acc Chem Res.* 1998;31:405–414; (b) Dietrich-Buchecker CO, Sauvage, JP. *Chem Rev.* 1987;87:795–810; (c) Faiz JA, Heitz V, Sauvage JP. *Chem Soc Rev.* 2009;38:422–442.
2. (a) van Dongen SFM, Elemans JAAW, Rowan AE, Nolte RJM. *Angew Chem Int Ed.* 2014;53:11420–11428; (b) Thordarson P, Bijsterveld EJA, Rowan AE, Nolte RJM. *Nature* 2003;424: 915–918; (c) Monnereau C, Hidalgo Ramos P, Deutman ABC, Elemans JAAW, Nolte RJM, Rowan AE. *J Am Chem Soc.* 2010;132:1529–1531.
3. Van Dongen SFM, Cantekin S, Elemans JAAW, Rowan AE, Nolte RJM. *Chem Soc Rev* 2014;43:99–122.
4. (a) Jiménez MC, Dietrich-Buchecker C, Sauvage JP, *Angew Chem Int Ed.* 2000;39:3284–3287; (b) Jimenez-Molero, MC, Dietrich-Buchecker C, Sauvage JP. *Chem Commun.* 2003;1613–1616; (c) Berná J, Leigh DA, Lubomska M, Mendoza SM, Pérez EM, Rudolf P, Teobaldi G, Zerbetto F. *Nat Mater.* 2005;4:704–710; (d) Ashcroft BA, Spadola Q, Qamar S, Zhang P, Kada G, Bension R, Lindsay S. *Small.* 2008;4:1468–1475; (e) Lussis P, Svaldo-Lanero T, Bertocco A, Fustin CA, Leigh DA, Duwez AS, *Nat Nanotechnol.* 2011; 6:553–557.
5. (a) Collier CP, Wong EW, Belohradský M, Raymo FM, Stoddart JF, Kuekes PJ, Williams RS, Heath JR. *Science.* 1999;285:391–394. (b) Cacialli F, Wilson JS, Michels JJ, Daniel C, Silva C, Friend RH, Severin N, Samori P, Rabe JP, O'Connell MJ, Taylor PN, Anderson HL, *Nat Mater.* 2002;1:160–164.
6. (a) Huang TJ, Brough B, Ho CM, Liu Y, Flood AH, Bonvallet PA, Tseng HR, Stoddart JF, Baller M, Magonov S. *Appl Phys Lett.* 2004;85:5391–5393; (b) Liu Y, Flood AH, Bonvallet PA, Vignon SA, Northrop BH, Tseng HR, Jeppesen JO, Huang TJ, Brough B, Baller M, *J Am Chem Soc.* 2005;127:9745–9759.
7. (a) Hsueh SY, Lai CC, Liu YH, Peng SM, Chiu SH. *Angew Chem Int Ed.* 2007;46:2013–2017; (b) Evans NH, Serpell CJ, Beer PD. *Chem. Commun.* 2011;47:8775–8777.

8. (a) Takashima Y, Osaki M, Ishimaru Y, Yamaguchi H, Harada A. *Angew Chem Int Ed.* 2011;50:7524–7528; (b) Blanco V, Carlone A, Hänni KD, Leigh DA, Lewandowski B, *Angew Chem Int Ed.* 2012;51:5166–5169. (c) Lewandowski B, De Bo G, Ward JW, Pappmeyer W, Kuschel S, Aldegunde MJ, Gramlich PM, Heckmann D, Goldup SM, D'Souza DM, Fernandes AE, Leigh DA, *Science.* 2011; 339:189–193. (d) van Dongen SFM, Clerx J, Nørgaard K, Bloemberg TG, Cornelissen JJLM, Trakselis MA, Nelson SW, Benkovic SJ, Rowan AE, Nolte RJM. *Nat Chem.* 2013;11:945–951.
9. Tuncel D, Steinke JHG. *Chem Commun.* 1999:1509–1510.
10. Crowley JD, Goldup SM, Lee AL, Leigh DA, McBurney RT. *Chem Soc Rev* 2009;38:1530–1541.
11. (a) Aucagne V, Berná J, Crowley JD, Goldup SM, Hänni KD, Leigh DA, Lusby PJ, Ronaldson VE, Slawin AMZ, Viterisi A, Walker DB. *J Am Chem Soc.* 2007;129:11950–11963; (b) Hänni KD, Leigh DA. *Chem Soc Rev.* 2009;39:1240–1251.
12. Berná J, Crowley JD, Goldup SM, Hänni KD, Lee AL, Leigh DA. *Angew Chem Int Ed.* 2007;46: 5709–5713.
13. (a) Elemans JAAW, Bijsterveld EJA, Rowan AE, Nolte RJM, *Chem Commun.* 2000;2443–2444; (b) Elemans JAAW, Bijsterveld EJA, Rowan AE, Nolte RJM, *Eur J Org Chem.* 2007;751–757.
14. (a) Coumans RGE, Elemans JAAW, Nolte RJM, Rowan AE. *Proc Natl Acad Sci USA.* 2006;103: 19647–19651; (b) Deutman ABC, Monnereau C, Elemans JAAW, Ercolani G, Nolte RJM, Rowan AE. *Science.* 200; 322:1668–1671; (c) Hidalgo Ramos P, Coumans RGE, Deutman ABC, de Gelder R, Smits JMM, Elemans JAAW, Nolte RJM, Rowan AE. *J Am Chem Soc.* 2007;129: 5699–5702; (d) Deutman ABC, Cantekin S, Elemans JAAW, Nolte RJM, Rowan AE. *J Am Chem Soc* 2014;136:9165–9172; (e) Cantekin S, Markvoort AJ, Elemans JAAW, Rowan AE, Nolte RJM, *J Am Chem Soc* 2015;137:3915–3923.
15. (a) Xia QH, Ge HQ, Ye CP, Liu ZM, Su KX. *Chem Rev.* 2005;105:1603–1662 (b) Wang C, Shalyaev KV, Bonchio M, Carofiglio T, Groves JT. *Inorg Chem.* 2006;45: 4769–4782; (c) Berkessel A, Ertürk E, Kaiser P, Klein A, Kowalczyk RM, Sarkar B. *Dalton Trans.* 2007;3427–3434.
16. Zhou CY, Huang JS, Che CM. *Synlett.* 2010;2681–2700.

17. Maas G. *Chem Soc Rev.* 2004;33:183–190.
18. Zhang JL, Che CM. *Org Lett.* 2002;4:1911–1914.
19. Galardon E, Le Maux P, Simonneaux G. *Tetrahedron.* 2000;56:615–621.
20. Galardon E, Roué S, Le Maux P, Simonneaux G. *Tetrahedron Lett.* 1998;39:2333–2334.
21. Zhou CY, Yu WY, Che CM. *Org. Lett.* 2002;4:3235–3238.
22. Chen Y, Huang L, Ranade MA, Zhang XP. *J Org Chem.* 2003;68:3714–3717.
23. (a) Collman JP, Rose E, Venburg GD, *J Chem Soc Chem Commun.* 1993;934–935. (b) Li GY, Che CM. *Org Lett.* 2004;6:1621–1623.
24. (a) Clemens RJ, Hyatt JA, *J Org Chem.* 1985;50: 2431–2435; (b) Clemens RJ, Witzeman, JS. *J Am Chem Soc.* 1989;111:2186–2193.
25. Elemans JAAW, Claase MB, Aarts PPM, Rowan AE, Schenning APHJ, Nolte RJM, *J Org Chem.*, 1999;64:7009–7016.
26. Slebodnick C, Seok WK, Kim K, Ibers A. *Inorg Chim Acta.* 1996;243:57–65.